REFORECASTS, AN IMPORTANT DATA SET FOR IMPROVING WEATHER PREDICTIONS

Thomas M. Hamill, [1] Jeffrey S. Whitaker, [1]
and Steven L. Mullen [2]

[1] *NOAA-CIRES Climate Diagnostics Center, Boulder, CO*

[2]*Institute of Atmospheric Physics, University of Arizona, Tucson, AZ*

19 May 2005

Submitted to *Bulletin of the American Meteorological Society*

Corresponding author address: Dr Thomas M Hamill, NOAA-CIRES Climate Diagnostics Center, Boulder, CO 80305-3328. E-mail: tom.hamill@noaa.gov
Phone 1 (303) 497-3060

ABSTRACT

A “reforecast” (retrospective forecast) data set has been developed. This data set is comprised of a 15-member ensemble run out to two weeks lead. Forecasts have been run every day from 0000 UTC initial conditions from 1979 to present. The model is a 1998 version of the National Centers for Environmental Prediction’s Global Forecast System (NCEP GFS) at T62 resolution. The 15 initial conditions consist of a reanalysis and seven pairs of bred modes.

This data set facilitates a number of applications that were heretofore impossible. Model errors can be diagnosed from the past forecasts and corrected, thereby dramatically increasing forecast skill. For example, calibrated precipitation forecasts over the United States based on the 1998 reforecast model are more skillful than precipitation forecasts from the 2002, higher-resolution version of the NCEP GFS. Other applications are also demonstrated, such as the diagnosis of bias for model development and an identification of the most predictable patterns of week 2 forecasts.

It is argued that the benefits of reforecasts are so large that they should become an integral part of the numerical weather prediction process. Methods for integrating reforecast approaches without seriously compromising the pace of model development are discussed.

Users wishing to explore their own applications of reforecasts can download them through a web interface.

CAPSULE SUMMARY:

Reforecasts (retrospective forecasts from the same model used operationally) can dramatically improve forecast skill through the statistical correction of the current forecast using the older forecasts.

1. Introduction

Reanalyses such as the National Centers for Environmental Prediction/National Center for Atmospheric Research (NCEP/NCAR) reanalysis (Kalnay et al. 1996) and the European Centre for Medium Range Weather Forecasts (ECMWF) 40-year reanalysis (ERA-40; Uppala et al. 2004) have become heavily used products for geophysical science research. These reanalyses run a practical, consistent data assimilation and short-range forecast system over a long period of time. While the observation type and quality may change somewhat, the forecast model and assimilation system are typically fixed. This facilitates the generation of a reanalysis data set that is fairly consistent in quality over time. These reanalysis data sets have facilitated a wide range of research; for example, the Kalnay et al. article above has been cited more than 3200 times.

In this article we explore the value of a companion data set to reanalyses, which we shall call "reforecasts." These are retrospective weather forecasts generated with a fixed numerical model. Model developers could use them for diagnosing model bias, thereby facilitating the development of new, improved versions of the model. Others could use them as data for statistically correcting weather forecasts, thereby developing improved, user-specific products (e.g., Model Output Statistics, or "MOS," Glahn and Lowry 1972, Carter et al. 1989). Others may use them for studies of atmospheric

predictability. Unfortunately, extensive sets of reforecasts are not commonly produced, utilizing the same model version as is run operationally. These computationally expensive reforecasts are "squeezed out" by operational data assimilation and forecast models run at as fine a resolution as possible.

Would the additional forecast improvement and diagnostic capability provided by reforecasts make them worth the extra computational resources they require? To explore this, we recently generated a prototype 25-year, 15-member ensemble reforecast data set using a 1998 version of the NCEP MRF model run at T62 resolution – admittedly a resolution far from state-of-the-art in operational numerical weather prediction centers in 2005. Despite the coarse resolution of this data set, we were able to make probabilistic week 2 forecasts that were more skillful than the operational NCEP forecasts based on higher-resolution models (Hamill et al. 2004). Others have also demonstrated the utility of reforecasts for improving predictions. Rajagopalan et al. (2002) and Stefanova and Krishnamurti (2002) used multimodel reforecasts to improve seasonal predictions, and Vitart (2004) demonstrated improved monthly forecasts using a smaller reforecast data set. Other smaller reforecast data sets also have been produced as companions to reanalysis data sets but have not been used for real-time statistical corrections of forecasts (Kistler et al. 2001 and Mesinger et al. 2005). The novelty of the reforecast data set discussed here is its length (every day, from 1979 to current), the ongoing production of real-time numerical forecasts from the same model, and that it is an ensemble of forecasts rather than a single integration.

A variety of other approaches are being explored for improving probabilistic forecasts. The "DEMETER" project in Europe has generated probabilistic seasonal

climate forecasts in a multi-model environment (Palmer et al. 2004, Hagedorn et al. 2005, Doblas-Reyes et al. 2005). Statistical approaches to correcting weather forecasts have been tried using shorter training data sets, including some with multi-model or multi-analysis approaches (Vislocky and Fritsch 1995, 1997, Hamill and Colucci 1997, 1998, Eckel and Walters 1998, Krishnamurti et al. 1999, Roulston and Smith 2003, Raftery et al. 2005, Wang and Bishop 2005). Results presented here will reinforce our previous assertion (Hamill et al. 2004) that for many difficult problems such as long-lead forecasts, forecasts of rare events, or forecasts of surface variables with significant bias, a large training sample size afforded by reforecasts may prove beneficial.

Our intent in this article is to introduce the reader to the several applications of reforecast data that demonstrate the potential for improving weather predictions and increasing our understanding of atmospheric predictability. We also intend to stimulate a serious discussion about the value of reforecasts. Is the value added so large that operational weather forecast centers should make reforecasting a regular part of the operational numerical weather prediction process? We will demonstrate that for the problem of probabilistic precipitation forecasting, there is a large, additional amount of skill that can be realized through the use of the reforecasts. Because reforecasting using higher-resolution models can be expensive, implementing this idea could require the purchase or reallocation of computer resources. Thus the implementation of reforecasting requires discussion at the top levels of the weather services.

We will provide a description of this data set in section 2 and illustrate how users can download raw data. We then demonstrate a range of potential applications in section 3, illustrating how such data sets may be used to inform a variety of forecast problems.

Section 4 discusses how reforecasts may be able to be integrated into operational NWP facilities without excessive disruption.

2. **Description of the reforecast data set.**

A T62 resolution (roughly 200 km grid spacing) version of NCEP's Global Forecasting System (GFS) model (Kanamitsu 1989; Kanamitsu et al. 1991; Hong and Pan 1996, Wu et al. 1997, Caplan et al. 1997, and references therein) was used with physics that were operational in the 1998 version of the model. This model was run with 28 vertical sigma levels. The reforecasts were generated at the NOAA lab in Boulder, Colorado, and real-time forecasts are now generated at NCEP and archived in Boulder.

A 15-member ensemble was produced every day from 1979 to current, starting from 0000 UTC initial conditions. The ensemble initial conditions consisted of a control initialized with the NCEP-NCAR reanalysis (Kalnay et al. 1996) and a set of 7 bred pairs of initial conditions (Toth and Kalnay 1993, 1997) re-centered each day on the reanalysis initial condition. The breeding method was the same as that used operationally in January, 1998. The forecasts extend to 15 days lead, with data archived every 12 h.

Because of the large size of this data set, we have chosen to archive only a limited set of model output. Winds, temperature, and geopotential height are available at the 1000, 850, 700, 500, 250, and 150 hPa levels. 10-m wind components, 2-m temperature, mean sea-level pressure, accumulated precipitation, convective heating, precipitable water, and 700 hPa relative humidity were also archived. Data can be downloaded using the online web form http://www.cdc.noaa.gov/reforecast/ (Fig. 1). Real-time data can also be ftp'ed from ftp://ftp.cdc.noaa.gov/Datasets.other/refcst/ensdata/yyyymmddhh,

where yyyy is the year, mm is the month, dd is the day, and hh is the hour of the initialization time. The real-time forecasts are typically available about 10 hours after initialization time.

3. **Some applications of the reforecast data set**.

As reanalyses have fostered many creative diagnostic studies, a long reforecast data set permits an examination and correction of weather forecasts in ways that were not previously possible. Robust statistical forecast techniques can be developed, the characteristics of model biases more thoroughly understood, and predictability issues explored. We demonstrate some interesting applications.

a. Forecasting with observed analogs.

Many forecast users desire reliable, skillful *high-resolution* ensemble predictions, perhaps for such applications as probabilistic quantitative precipitation forecasting or hydrologic applications (e.g., Clark and Hay 2004). The data set produced in this pilot reforecast project is comparatively low resolution, T62. However, it may be possible to downscale and correct systematic errors in ensemble forecasts through analog techniques, producing a skillful probabilistic forecast at as high a resolution as the observed data. Given a long time series of reforecasts and high-resolution analyses or observations, a two-step procedure is invoked. First, today's ensemble forecast is compared to reforecasts of the same lead. Second, the dates of the closest pattern matches are noted, and an ensemble is formed from the observed or analyzed conditions on those dates.

This two-step procedure may be appealing, for it simulates the forecast process of many humans: we look at the current forecast, recall situations where the forecast

depiction was comparable (step 1), and try to recall the weather that actually occurred (step 2). Analog forecast techniques have a rich history (e.g., Toth 1989, van den Dool 1989, Livezey et al. 1994, Zorita and von Storch 1999, Sievers et al. 2000), but most utilize a simpler approach of directly finding observed analogs to the forecast. Consider a situation where the forecast model is consistently too wet. In a one-step analog technique, the ensemble of observed analogs would, by construction, retain the forecast's wet bias. The two-step procedure would first find similar forecasts, but if the observed data were drier, the second step would compensate for the wet bias.

To demonstrate the potential of this two-step analog procedure, the technique was used to generate probabilistic forecasts of 24-h accumulated precipitation over the conterminous United States (US). Forecasts were verified during January-February-March 1979-2003 (JFM 79-03). Approximately 30-km North American Regional Reanalysis (NARR; Mesinger et al. 2005) analyzed precipitation data was used both for verification and as the data set from which historical observed weather analogs were selected.

The first step of the procedure was to find the closest *local* reforecast analogs to the current numerical forecast. That is, within a limited-size region, today's forecast was compared against past forecasts in that same region and at the same forecast lead. Specifically, the ensemble-mean precipitation forecast pattern was computed at a subset of 16 coarse-resolution grid points (for example, the blue dots in Fig. 2).[1] The ensemble-

[1] Techniques that attempted to find analogs for each member were less skillful; we believe that this is both because the ensemble mean acts as a filter of the unpredictable

mean forecast in this region were compared to ensemble mean reforecasts over all other years, but only those within a window of 91 days (+ / - 45 day window) around the date of the forecast. For example, a 15 February 2002 4-day ensemble-mean forecast over the northwest US was compared against the 4-day ensemble mean reforecasts from 1 January – 1 April 1979 - 2001 over the northwest US. The root-mean square (RMS) difference between the current forecast and each reforecast was computed, averaged over the 16 grid points in Fig. 1. The *n* historical dates with the smallest RMS difference were chosen as the dates of the analogs.

The second step was the collection of the ensemble of observed weather on the dates of the closest *n* analogs. For this application, the NARR observed precipitation states were collected at the interior red dots in Fig. 2. A probabilistic forecast was then generated using the ensemble relative frequency; for example, if 2/3 of the members at a grid point had greater than 10 mm accumulated rain, the probability of exceeding 10 mm was set to 67%.

The process was then repeated for other locations around the US. A full, high-resolution probabilistic forecast was generated by tiling together the local analog forecasts.[2]

---

scales and because there is not much relationship between spread and skill in this particular ensemble (Hamill et al. 2004).

[2] Tiling can in some situations introduce slight discontinuities of the probabilities at the boundaries between tiles. We tested a slightly modified method whereby larger, overlapping tiles were used, and the final probabilities were increasingly averaged toward the edges of the tiles. This produced a smoother field, though the skill scores were slightly diminished.

Figure 3 shows the data from one such case, a 3-day heavy precipitation event along the west coast in late December, 1996 (Ralph et al. 1998, Ogston and Hay 2000). Figure 3a shows the probabilistic forecasts generated from the raw T62 ensemble. Regions where the ensemble forecast members exceeded 100 mm of rainfall over the two days excluded Washington State, and the probabilities of greater than 100 mm were highest in northern California. In comparison, when probabilities were computed from the n=75 historical analogs, nonzero probabilities for exceeding 100 mm were extended north into Washington State. The high probability tended to be localized more along the coastal mountain ranges, the Cascades, and the Sierra Nevada range. The observed precipitation (Fig. 3c) shows that the heaviest precipitation had a similar spatial pattern of high probabilities, with heaviest precipitation along the mountain ranges.

To understand better how the analog technique performed, consider the forecasts at the three dots in Fig. 3a. The lower two dots, near Mt. Shasta (bottom) and Medford, Oregon (middle) were both in the region where the model predicted record rainfall. The top dot, in the Olympic Range in Washington, was outside of the region where any of the ensemble members forecast over 100 mm (precipitation was forecast there, just consistently less than 100 mm). At these three grid points, we will consider the raw ensemble data at that grid point, the values of the ensemble means of the chosen forecast analogs interpolated to this location, and the values of the associated observed data on those same days. Figure 4a provides information for the grid point near Mt. Shasta. The histogram along the top denotes the raw T62 ensemble forecast information, showing that the precipitation was exceptionally heavy at this point for all ensemble members. The scatterplot shows the closest 75 ensemble-mean reforecast values of rainfall (abscissa)

plotted against the associated 75 historical NARR analyzed rainfall values (ordinate). The histogram for the NARR analog ensemble is plotted along the right-hand side. As indicated by the difference in the position of the raw forecast histogram and forecast analogs dots, the reforecast data was not able to find many close forecast analogs to this record event, at least considering just the data at this one point. However, the observed amounts associated with even these relatively poor analogs often indicated heavier precipitation than forecast, correcting a typical under-forecast bias. Also, the spread of the observed analogs was much larger than the spread of the raw ensemble or the ensemble-mean forecast analogs, correcting the ubiquitous precipitation spread deficiency (e.g., Hamill and Colucci 1997, Mullen and Buizza 2001).

In Fig. 4b, the raw forecast ensemble at Medford, Oregon also indicated a record-breaking heavy precipitation event. As with Mt. Shasta, no similarly wet analogs could be found among the reforecasts. However, this location was in a climatological rain shadow of the Coast Ranges in Oregon and California. The smoothed terrain in the reforecast model was unable to resolve this level of terrain detail, so heavier precipitation than observed was commonly forecast in Medford. Consequently, the two-step analog procedure adjusted for the typical over-forecast bias. The very different bias corrections between Mt. Shasta and Medford amount to a way of downscaling the coarse forecast to be consistent with the local variations of rainfall in the observed data.

In Fig. 4c, moderate precipitation amounts were forecast in the original ensemble in the Olympic Range of Washington State, and many similar reforecast analogs were found in the data set. The associated NARR observed analogs tended to be heavier in

amount, with a larger spread than the original ensemble, thus correcting for an under-forecasting bias and what was probably insufficient spread in the original ensemble.

The analog technique apparently can correct for bias and spread deficiencies and downscale the forecast to account for terrain effects. But does the skill of this technique exceed that from existing operational ensemble forecasts? To determine this, we have extracted the operational ensemble forecasts from NCEP for JFM 02-03; starting in January 2002, NCEP GFS ensemble forecasts were computed at T126 resolution to 84 h lead, providing it with a resolution advantage over the reforecast model. Figures 5a-b show the Brier Skill Score (Wilks 1995) of ensemble forecasts at the 2.5 mm and 25 mm (per 24 h) thresholds, respectively, calculated in a way that does not exaggerate forecast skill (Hamill and Juras 2005). The 75-member analog reforecast technique is much more skillful than the NCEP forecast, especially at the 25 mm threshold.

The increase in skill is primarily due to an increase in the resolution of the probability forecasts rather than improved reliability. Resolution measures the ability of the forecasts to distinguish between situations with different observed event frequencies (Murphy 1973, Wilks 1995); higher numbers indicate more skill. Reliability indicates how closely the long-term observed event frequency given a forecast probability matches the forecast probability; the smaller the reliability value the better (ibid). If the climatological probability of event occurrence is the same for all samples (Hamill and Juras 2005), then the Brier skill score (*BSS*) can be decomposed as

$$BSS = \frac{resolution - reliability}{uncertainty}, \qquad (1)$$

(Wilks 1995, eq. 7.29), where uncertainty denotes the variability of the observations (see Wilks for formal definitions). Figure 6 shows the *BSS* decomposition for the event of 24-

h accumulated precipitation larger than the upper quintile of the climatological distribution for both NCEP forecasts and 75-member analog forecasts, using only points where the climatological probability of precipitation is greater than 20 percent (otherwise the definition of the upper quintile is ambiguous). Reliability is improved through the application of the analog technique, but most of the increase in the *BSS* is a result of increased resolution.

The increased skill of the analog forecasts relative to operational NCEP forecasts results suggest that there is some benefit from the use of analogs, the large training data set, or both. Figure 4 demonstrated how the use of high-resolution observed analogs permitted the extraction of small-scale detail that was not in the original forecast. But are two-plus decades of reforecasts necessary? Figure 7 indicates that forecast skill is degraded somewhat when shorter training data sets are used, especially at high precipitation thresholds. In these cases, when a large amount of rain is forecast, it is important to have other similar high-rain forecast events in the data set, otherwise very few close analogs can be found. For 2.5 mm forecast amounts, where there are many similar analogs in the reforecast data set, and little skill is gained between 3 and 24 years of training data. However, for 25 mm, there still is a notable increase in skill between 3 and 24 years, indicating the potential benefit of the long training data set with this technique. Notice also in Figure 7 that the ensembles of different sizes were tested, and relatively small ensembles provided the most skill at short leads and larger ensembles at long leads. When required to use short training data sets, it is difficult to find many close analogs for these short-lead forecasts, so the performance is degraded if too many analogs

are used to set probabilities. For large training data sets, the performance difference at short leads is minimal between 25 and 75 members (not shown).

Figure 8 shows the spatial pattern of the 75-member analogs' *BSS* at 2.5 mm and 4 days lead. Skill varied greatly with location. The method produces highly skillful forecasts along the West Coast, presumably because the methodology provides a way of downscaling the weather appropriate to the complex terrain. Forecast skill was generally high over the eastern US and lower over the northern US and Rockies. In general, the *BSS* tended to be smaller in drier regions, where the reference climatology forecasts were more skillful. Also, the skill appeared to be less in regions where precipitation tended to fall as snow, perhaps because the observational data was less trustworthy (both the radar and gage data used in the NARR precipitation analysis are less accurate in snow). In any case, the forecasts are generally quite reliable (Fig. 6), though less so at short forecast leads, where there is a tendency to under-forecast probabilities[3].

Analog techniques will never predict record-setting events, events that lie outside the span of the past data. If predicting extreme events is of primary importance, other calibration techniques may prove more useful. Also, as Lorenz (1969) noted, it is impossible to find *global* analogs for the current weather during a span of time as long as the recorded history of the atmosphere. Hence, analogs must be found and applied only

[3] This is because there tend to be more light forecast precipitation events than heavier ones among the reforecasts, so the technique more commonly finds close analogs with slightly lighter forecast amounts than heavier amounts. At short leads, there is skill in the raw numerical forecast; the observed precipitation associated with the forecast analogs with lighter amounts tends to be smaller than the observed precipitation associated with forecast analogs with larger amounts. Hence, the observed ensemble has a dry bias. It is possible to choose analogs based upon the closeness of the *rank* of the precipitation forecast relative to the sorted reforecasts, so that there are as many analogs with heavier forecast precipitation as with lighter precipitation. These forecasts are more reliable and slightly more skillful. We expect to document this technique in a subsequent manuscript.

in geographically limited regions, so that the difference between the current forecast and a past forecast analog is a small fraction of the climatological forecast variance. Still, analog techniques should have very notable advantages. They represent a conditional climatology given the forecast. Hence, they should commonly have positive skill relative to the overall climatological forecast. This is a property that raw forecasts from most numerical models commonly do not exhibit. It is more typical for them to drift to a climatological distribution different from the observed distribution, so that longer-lead forecasts exhibit a skill worse than climatology. Analog techniques also can be tailored to a wide range of user problems. For example, suppose a user requires probabilistic wind forecasts at a wind turbine. If a large data set of past observations of wind at the turbine site is available, the basic technique can be repeated: find an ensemble of past forecast days where the meteorological conditions were similar to today's forecast, produce a probabilistic forecast from the associated observed winds on the days of the analogs. For another recent work on forecast analogs using this reforecast data set for hydrologic applications, see Gangopadhyay et al. (2004).

The analog technique demonstrated here is a proof of concept. The technique can be improved in some respects, and the technique is also not a cure-all for all weather forecast problems. If systematic errors are smaller, as they may be when, say, forecasting 500 hPa geopotential, it is unlikely that statistical corrections of an older model will render the forecasts more skillful than those from newer, higher-resolution models (personal communication, Z. Toth). Still, for many of the problems that users most care about – precipitation, surface temperature, wind speed – model biases can be large and reforecasts may prove to be a significant aid. The lessons here were that a simple

statistical correction technique in conjunction with low-resolution reforecasts was able to produce probabilistic precipitation forecasts exceeding the skill of the higher-resolution NCEP global ensemble forecast system, and the long length of the reforecast training data set was apparently helpful in achieving this skill improvement.

This reforecast data and this particular application may be useful to others that are developing and testing new ensemble calibration methods. The precipitation forecast and observed data used in this section is freely available to the public, along with sample code for reading the data. We encourage others to explore this data set and to compare their results against our own. The data and code can be downloaded from http://www.cdc.noaa.gov/reforecast/testdata.html.

b. *Diagnosing model bias from reforecasts.*

Suppose a model developer wanted to know the long-term mean bias of a particular variable in the forecast model, where bias is the mean forecast minus the mean verification. Reforecasts are a useful tool for diagnosing this. For example, Fig. 9a shows the bias of 850 hPa temperature forecasts at a location near Kansas City, Missouri. These biases were calculated by subtracting the NCEP-NCAR analyses from the ensemble-mean forecasts using 1979-2001 data and a 31-day window centered on the day of interest. There is a large cold bias at shorter lead times in the winter and warm biases in late summer, especially at longer leads. And though not shown here, different locations have very different bias characteristics; for example, near San Francisco, there is a strong cold bias at longer leads during mid-summer.

Can the long-term bias be properly estimated from a much shorter data set of reforecasts? Figure 9b suggests that often they cannot. This panel shows the standard deviation of the yearly bias estimates. To generate this figure, the bias was estimated for each year, day, and forecast lead using just a 31-day window centered on the day of interest. From the 23 bias estimates from 1979 to 2001, the standard deviation was calculated and plotted. Note that the standard deviation grows with increasing forecast lead and is generally larger in the winter than in the summer. This is due to the larger variability of the forecasts during the wintertime at longer leads. At most forecast leads and times of the year the spread in the yearly bias estimate is larger than the magnitude of the bias in Fig. 9a. For a numerical modeler, this indicates that the long-term average bias is liable to be misestimated using a single year of data, especially at long leads.

c. *Studying predictability using reforecasts*.

Forecasts of individual weather systems during the first week are generally referred to as "weather" forecasts, the skill of which requires an accurate initial condition. Long-lead predictions, such as those associated with El-Nino/Southern Oscillation (ENSO) are generally referred to as "climate" forecasts, and their skill is primarily driven by to sensitivity to boundary conditions such as sea-surface temperatures. In between these two extremes lies the boundary between weather and climate forecasts, in which individual weather systems may not be predictable, but larger-scale flow patterns which influence those weather systems may retain some sensitivity to initial conditions and may also be influenced by persistent boundary forcing. The phenomena that yield skill in the second week of an ensemble forecast are generally large scale and low frequency, and

hence there may be only a few independent samples of these events each season. In addition, the predictable signal may be small compared to the uncertainty in a single forecast, so ensembles may be needed to extract that signal. Quantifying the nature of the predictable signal in week two therefore requires a large sample of ensemble forecasts, spanning many years. The reforecast data set is one of the first to satisfy these requirements. Very basic questions, like "how much skill is there in week 2?" and "where does that skill come from?" remain largely unanswered. In this section we show a few simple diagnostics using the reforecast data set which provide some insight into these questions. They illustrate the utility of the reforecast data set in investigations of atmospheric predictability.

Figure 10 shows a map of the temporal correlation between the time series of ensemble mean forecast and observed 500 hPa height for all day 10 forecasts in the reforecast data set initialized during December-February 1979-2003. Values locally exceeded 0.6 in the central Pacific, while the hemisphere average was 0.47. While these values may seem low, they do indicate that skillful probabilistic forecasts are possible at day 10. Hamill et al. (2004, Fig. 6d) showed that a correlation of 0.5 can be translated into a Ranked Probability Skill Score of 0.15 for terciles of the climatological probability distribution; small, but useful.

What are the skillfully predicted patterns in these day-10 forecasts? To answer this question, we have performed a statistical analysis of the 25-year data set of wintertime day-10 500 hPa height forecasts in order to identify the most predictable patterns. The technique used was Canonical Correlation Analysis (CCA; Bretherton et al., 1992), which seeks to isolate the linear combination of data from a predictor field and

the linear combination of data from a predictand field that have the maximum linear correlation. The analysis was performed in the space of the truncated principal components, or PCs (Barnett and Preisendorfer, 1987). Here the predictor field consisted of the leading 20 PCs of ensemble-mean week two forecast 500 hPa height, while the predictand field consisted of the leading 20 PCs of the corresponding weekly mean verifying analyses. The analysis was similar in spirit to that performed by Renwick and Wallace (1995), using 14 years of day-10 forecasts from the European Centre for Medium-Range Weather Forecasts. Although their 'most predictable pattern' is very similar to the one shown here, interpretation of their results was hampered by the fact that the forecasts were from a single deterministic run (not an ensemble) and there were significant changes in the forecast model over the span of their forecast archive.

Figure 11 shows the three most predictable patterns identified by the CCA analysis for day-10 forecasts, while Figure 12 shows the correlation between the time series of these patterns as a function of forecast lead. The patterns were computed for day-10 forecasts, but we have projected the forecasts for all other forecast leads on to these same patterns to see how the forecast skill evolves during the forecast period. The most predictable patterns are similar to well-known recurring persistent circulation anomalies, often called 'teleconnection patterns' (Barnston and Livezey, 1987). The first pattern is similar to the Tropical/Northern Hemisphere pattern, so named by Mo and Livezey (1986), which are often observed to appear in Northern Hemisphere wintertime seasonal means during El Nino/Southern Oscillation (ENSO) events. Indeed, the model forecast tropical precipitation during the first week regressed on the time series of this pattern (not shown) shows a significant relationship between precipitation in the central

equatorial Pacific and the amplitude of the most predictable pattern at day 10. However, values of this correlation were less than 0.3, indicating that only a modest fraction of the variance of this pattern in day 10 forecasts is directly related to variations in tropical convection. The second most predictable pattern was similar to the Pacific/North American pattern (Wallace and Gutzler, 1981), while the third resembled the classical North Atlantic Oscillation (ibid). Regression analysis shows that neither of these patterns had a strong relationship with the model forecast precipitation in equatorial regions during week one, implying that slow variations in tropical convection were not primarily responsible for their predictability. The ability of the ensemble system to forecast these patterns is remarkable, with correlation skill exceeding 0.7 at day 10 for all three patterns, and skill exceeding 0.6 at day 15 for the most predictable pattern. The skill of a forecast which simply persists the projection of these patterns in the 1 day forecast to day 10 is much lower than the actual 10 day forecast from the ensemble system (Figure 12), indicating the forecast model is skillfully predicting the tendency of these patterns during the first week of the forecast. Diagnosing the mechanisms responsible for the skillful prediction of the those tendencies is beyond the scope of this article, but would certainly be a likely candidate for further research using this dataset.

These results show that the reforecast data set provides a new opportunity to address basic predictability questions which were previously out of reach due to the sample size limitations and questions concerning the impact of model changes in existing operational forecast data sets.

4. **How can reforecasts be integrated into operational numerical weather prediction?**

This paper has demonstrated some of the benefits of "reforecasts," a companion data set to reanalyses. As with reanalyses, a fixed model is used, and forecasts for retrospective cases are computed with the fixed model. Use of reforecasts improved probabilistic precipitation forecasts dramatically, aided the diagnosis of model biases, and provided enough forecast samples to answer some interesting questions about predictability in the forecast model.

Weather prediction facilities like the Environmental Modeling Center at NCEP already totally utilize the available computational resources, and planned model upgrades will utilize most of the newly available resources in the near future. How then can reforecasts be integrated into operational numerical weather prediction?

One possible interim solution is that the reforecasts could be run with a less than state-of-the-art version of the forecast model. Our results suggest that substantial forecast improvements were possible even with the T62 model output. Consider then the scenario where the "flagship" product at the weather production facility is a 50-level, 50-member global ensemble of a T300 model. The operational production of a 25-level, 25-member, T150 forecast could be produced at 1/64 the computational expense of the flagship product. Hence, if 16 years of reforecasts were computed, this would require computer resources equivalent to producing the operational forecasts for 3 months. If the companion reforecasts were computed offline on another computer, then the reforecast computations would barely affect operations. We suggest that this is an appropriate,

conservative model to follow in the near future. A timely forecast would be generated from a fixed, reduced-resolution version of the model, one where a companion reforecast data set had been generated. Forecast products would be generated through statistical techniques such as those demonstrated here, and the reforecast-based products would be compared to products based on the flagship product. If they were deemed to improve weather forecast capabilities, then every few years the reforecast would be updated, utilizing a newer, improved version of the forecast model at higher resolution, maintaining the same relative usage of operational CPU resources relative to the updated flagship product.

Computing reforecasts is a task that is easily parallelized, so it can take advantage of massively parallel clusters of inexpensive computers. Individual ensemble member forecasts can be computed on different processors in the cluster, and forecasts for many different initial times can also be parallelized. The cluster of personal computers and storage array used in this experiment cost approximately $90,000, a tiny fraction of the cost of the NCEP's supercomputers.

Acknowledgments

T. Hamill's contribution was partially supported under National Science Foundation grants ATM-0120154 and ATM-0205612. We thank Xue Wei and Andres Roubicek for their help in processing the voluminous data used in this study. We thank three anonymous reviewers for their constructive criticism.

References

Barnston, A. G., and R. E. Livezey. 1987: Classification, seasonality and persistence of low-frequency atmospheric circulation patterns. *Mon. Wea. Rev.,* **115**, 1083–1126.

Barnett, T. P., and R. Preisendorfer, 1987: Origins and levels of monthly and seasonal forecast skill for United States surface air temperatures determined by canonical correlation analysis. *Mon. Wea. Rev*., **115**, 1825–1850.

Bretherton C. S., C. Smith and J. M. Wallace. 1992: An intercomparison of methods for finding coupled patterns in climate data. *J. Clim*., **5**, 541–560.

Caplan, P., J. Derber, W. Gemmill, S.-Y. Hong, H.-L. Pan, and D. Parrish, 1997: Changes to the 1995 NCEP operational medium-range forecast model analysis-forecast system. *Wea. Forecasting*, **12**, 581-594.

Carter, G. M., J. P. Dallavalle, and H. R. Glahn, 1989: Statistical forecasts based on the National Meteorological Center's numerical weather prediction system. *Wea. Forecasting*, **12**, 581-594.

Clark, M. P., and L. E. Hay, 2004: Use of medium-range numerical weather prediction model output to produce forecasts of streamflow. *J. Hydrometeor*., **5**, 15-32.

Doblas-Reyes, F. J., R. Hagedorn, and T. N. Palmer, 2005: The rationale behind the success of multi-model ensembles in seasonal forecasting: Part II: calibration and combination. *Tellus*, in press.

Eckel, F. A., and M. K. Walters, 1998: Calibrated probabilistic quantitative precipitation forecasts based on the MRF ensemble. *Wea. Forecasting*, **13**, 1132-1147.

Gangopadhyay, S., M.P. Clark, B. Rajagopalan, K. Werner, and D. Brandon, 2004: Effects of spatial and temporal aggregation on the accuracy of statistically downscaled precipitation estimates in the Upper Colorado River basin. *Water Resources Research*, submitted.

Glahn, H. R., and D. A. Lowry, 1972: The use of model output statistics (MOS) in objective weather forecasting. *J. Appl. Meteor.*, **11**, 1203-1211.

Hagedorn, R., F. J. Doblas-Reyes, and T. N. Palmer, 2005: The rationale behind the success of multi-model ensembles in seasonal forecasting. Part I: basic concept. *Tellus*, in press.

Hamill, T. M., and S. J. Colucci, 1997: Verification of Eta-RSM short-range ensemble forecasts. *Mon. Wea. Rev.*, **125**, 1312-1327.

---------- , and ----------, 1998: Evaluation of Eta-RSM ensemble probabilistic precipitation forecasts. *Mon. Wea. Rev.*, **126**, 711-724.

----------, J. S. Whitaker, and X. Wei, 2004: Ensemble re-forecasting: improving medium range forecast skill using retrospective forecasts. *Mon. Wea. Rev.*, **132**, 1434-1447.

---------- , and J. Juras, 2005: Common forecast verification metrics can overestimate skill. *Mon. Wea. Rev.*, in review. Available from http://www.cdc.noaa.gov/people/tom.hamill/skill_overforecast.pdf .

Hong, S.-Y., and H.-L. Pan, 1996: Nonlocal boundary layer vertical diffusion in a medium-range forecast model. *Mon. Wea. Rev.,* **124**, 2322-2339.

Kalnay, E., and co-authors, 1996: The NCEP/NCAR 40-year reanalysis project. *Bull. Amer. Meteor. Soc.*, **77**, 437-472.

Kanamitsu, M., 1989: Description of the NMC global data assimilation and forecast system. *Wea. Forecasting*, **4**, 334-342.

---------- , and Coauthors, 1991: Recent changes implemented into the global forecast system at NMC. *Wea. Forecasting*, **6**, 425-435.

Kistler, R., E. Kalnay, W. Collins, S. Saha, G. White, J. Woollen, M. Chelliah, W. Ebisuzaki, M. Kanamitsu, V. Kousky, H. van den Dool, R. Jenne, and M. Fiorino. 2001: The NCEP–NCAR 50–Year Reanalysis: Monthly Means CD–ROM and Documentation. *Bull. Amer. Meteor. Soc*., **82**, 247–267.

Krishnamurti, T. N., and coauthors, 1999: Improved weather and seasonal climate forecasts from multimodel superensemble. *Science*, **285**, 1548-1550.

Livezey, R. E., A. G. Barnston, G. V Gruza, and E. Y. Ran'kova, 1994: Comparative skill of two analog seasonal temperature prediction systems: objective selection of predictors. *J Climate*, **7**, 608-615.

Lorenz, E.N., 1969: Three approaches to atmospheric predictability. *Bull. Amer. Meteor. Soc*., **50**, 345-349.

Mo, K.C and R. E. Livezey. 1986: Tropical-extratropical geopotential height teleconnections during the northern hemisphere winter. *Mon. Wea. Rev*., **114**, 2488–2515.

Mesinger, F., G. DiMego, E. Kalnay, P. Shafran, W. Ebisuzaki, D. Jovic, J. Woollen, K. Mitchell, E. Rogers, M. Ek, Y. Fan, R. Grumbine, W. Higgins, H. Li, Y. Lin, G. Manikin, D. Parrish, and W. Shi, 2005: North American Regional Reanalysis. *Bull. Amer. Meteor. Soc*., submitted.

Mullen, S. L., and R. Buizza, 2001: Quantitative precipitation forecasts over the United States by the ECMWF ensemble prediction system. *Mon. Wea. Rev.*, **129**, 638-663.

Murphy, A. H., 1973: A new vector partition of the probability score. *J. Appl. Meteor.*, **12**, 595-600.

Ogston, A., D. Cacchione, R. Sternberg, and G. Kineje, 2000: Observations of storm and river flood-driven sediment transport on the northern California continental shelf. *Continental Shelf Research*, **20**, 2141-2162.

Palmer, T. N., and others, 2004: Development of a European multimodel ensemble system for seasonal to interannual prediction (DEMETER). *Bull. Amer. Meteor. Soc.*, 85, 853-872.

Rajagopalan, B., U. Lall, and S. E. Zebiak, 2002: Categorical Climate Forecasts through Regularization and Optimal Combination of Multiple GCM Ensembles. *Mon. Wea. Rev.*, **130**, 1792–1811.

Raftery, A. E., T. Gneiting, F. Balabdaoui, and M. Polakowski, 2005: Using Bayesian model averaging to calibrate forecast ensembles. *Mon. Wea. Rev.*, in press.

Ralph, F.M., P.J. Neiman, P.O.G. Persson, and J.-W. Bao, 1998: Observations of California's New Year's Day Storm of 1997. *Preprints, 2nd AMS Conf. on Atmospheric and Oceanic Prediction and Processes*, 11-16 January, 1998, Phoenix, AZ, 219-224.

Renwick, J. A. and J. M. Wallace. 1995: Predictable anomaly patterns and the forecast skill of northern hemisphere wintertime 500-mb height fields. *Mon. Wea. Rev.*, **123**, 2114–2131.

Roulston, M. S., and L. A. Smith, 2003: Evaluating probabilistic forecasts using information theory. *Tellus*, **55A**, 16-30.

Sievers, O., K. Fraedrich, and C. Raible, 2000: Self-adapting analog ensemble predictions of tropical cyclone tracks. *Wea. Forecasting*, **18**, 3-11.

Stefanova, L., and T. N. Krishnamurti, 2002: Interpretation of seasonal climate forecast using Brier skill score, the Florida State University superensemble, and the AMIP-I dataset. *J. Climate*, **15**, 537-544.

Toth, Z., 1989: Long-range weather forecasting using an analog approach. *J. Climate*, **2**, 594-607.

----------, and E. Kalnay, 1993: Ensemble forecasting at NMC: The generation of perturbations. *Bull. Amer. Meteor. Soc*. **74**, 2317-2330.

----------, and ---------- , 1997: Ensemble forecasting at NCEP and the breeding method. *Mon. Wea. Rev*., **125**, 3297-3319.

Uppala, S. M., and coauthors, 2004: The ERA-40 reanalysis. *Quart. J. Roy. Meteor. Soc.*, submitted.

van den Dool, H. M., 1989: A new look at weather forecasting through analogues, *Mon. Wea. Rev*., **117**, 2230-2247

Vitart, F., 2004: Monthly forecasting at ECMWF. *Mon. Wea. Rev*., **132**, 2761-2779.

Wang, X., and C. H. Bishop, 2005: Improvement of ensemble reliability with a new dressing kernel. *Quart. J. Royal Meteor. Soc*., in press.

Wallace, J. M. and D. S. Gutzler. 1981: Teleconnections in the geopotential height field during the northern hemisphere winter. *Mon. Wea. Rev*., **109**, 784–812.

Wilks, D. S., 1995: *Statistical Methods in the Atmospheric Sciences*. Cambridge Press, 467 pp.

Wu., W., M. Iredell, S. Saha, and P. Caplan, 1997: Changes to the 1997 NCEP Operational MRF Model Analysis/Forecast System. NCEP Technical Procedures Bulletin 443, 22 pp. [Available online at http://www.nws.noaa.gov/om/tpbpr.shtml, and from Office of Services, NOAA, National Weather Service, 1325 East-West Highway, W/0551, Silver Spring, MD, 20910.

Zorita, E., and H. von Storch, 1999: The analog method as a simple statistical downscaling technique: comparison with more complicated methods. *J. Climate*, **12**, 2474-2489.

List of Figures

Figure 1: Screenshot of the reforecast data set download web page.

Figure 2: Map of reforecast grid points used in determination of closest analog forecasts. The smaller dots denote where NARR data is available (a 32 km Lambert Conformal grid). Large blue dots denote where the T62 forecasts are available (interpolated from a global 2.5 degree grid to every eighth NARR grid point). The analyzed fields associated with the closest pattern matches at the blue dots are extracted at the red dots. The national forecast is then comprised of a tiling of similar regions from around the country.

Figure 3: (a) Raw ensemble-based probability of greater than 100 mm precipitation accumulated during days 4-6 for a forecast initialized 0000 UTC 26 December 1996 (from 0000 UTC 29 December 1996 to 0000 UTC 1 January 1997). Dots indicate locations used in Fig. 4. (b) As in (a), but where probabilities have been estimated from relative frequency of historical NARR analogs. (c) Observed precipitation from NARR (mm). 100 mm threshold highlighted.

Figure 4: Ensemble forecast, reforecast analog, and observed analog data for three dots in Fig. 3a. Histograms along tops of plots indicate the raw T62 ensemble forecast total amounts. Histograms along right of plots indicate the frequency of NARR analog forecast amounts. Scatterplots indicate the joint value of ensemble-mean analog forecasts taken from the reforecast data set (abscissa) and the value of the associated NARR historical analog (ordinate). (a) Scatterplot from Mt. Shasta (northern California), (b)

scatterplot from Medford (southern Oregon), (c) scatterplot from Olympic Mountains, Washington.

Figure 5: Brier Skill Score of 75-member analog and NCEP ensemble forecasts measured relative to climatology. (a) 2.5 mm skill, (b) 25 mm skill.

Figure 6: Reliability and resolution (scaled by the uncertainty), and Brier Skill Score (BSS) of the probability of precipitation occurring in the upper quintile of the climatological distribution, both for NCEP and 75-member analog forecasts. The overall height of the bar for each day indicates the resolution, NCEP on the left and analogs on the right. NCEP reliability is colored blue, analog reliability is colored green, NCEP BSS is red, and analog BSS is yellow.

Figure 7: Brier Skill Scores of the analog reforecast technique for various lengths of the training data set.

Figure 8: Map of Brier Skill Scores of 24-h accumulated precipitation forecasts between 3 and 4 days lead at 2.5 mm threshold for JFM 1979-2002.

Figure 9: (a) 850 hPa temperature bias at -95.0 W, 40.0 N, as a function of time of year and forecast lead. (b) Standard deviation of the yearly bias estimates.

Figure 10: Correlation between time series of ensemble mean day-10 forecasts and corresponding verifying analyses (from the NCEP/NCAR reanalysis) at every grid point in the Northern Hemisphere for December to February 1979-2003.

Figure 11 : Ensemble mean day-10 forecast 500 hPa height regressed on to the time series of the three most predictable forecast patterns. Contour interval 15 m. The correlation of between the time series of the predictor pattern and the corresponding predictand pattern (*r*) is given for each pattern.

Figure 12: Correlation between the time series of the first three most predictable 500 hPa height day 10 forecast patterns and the time series of the corresponding patterns in the verifying analyses as a function of forecast lead time. The three dots labeled 'persistence forecast' indicate the skill of a forecast which persists the projections in the day 1 forecast to day 10.

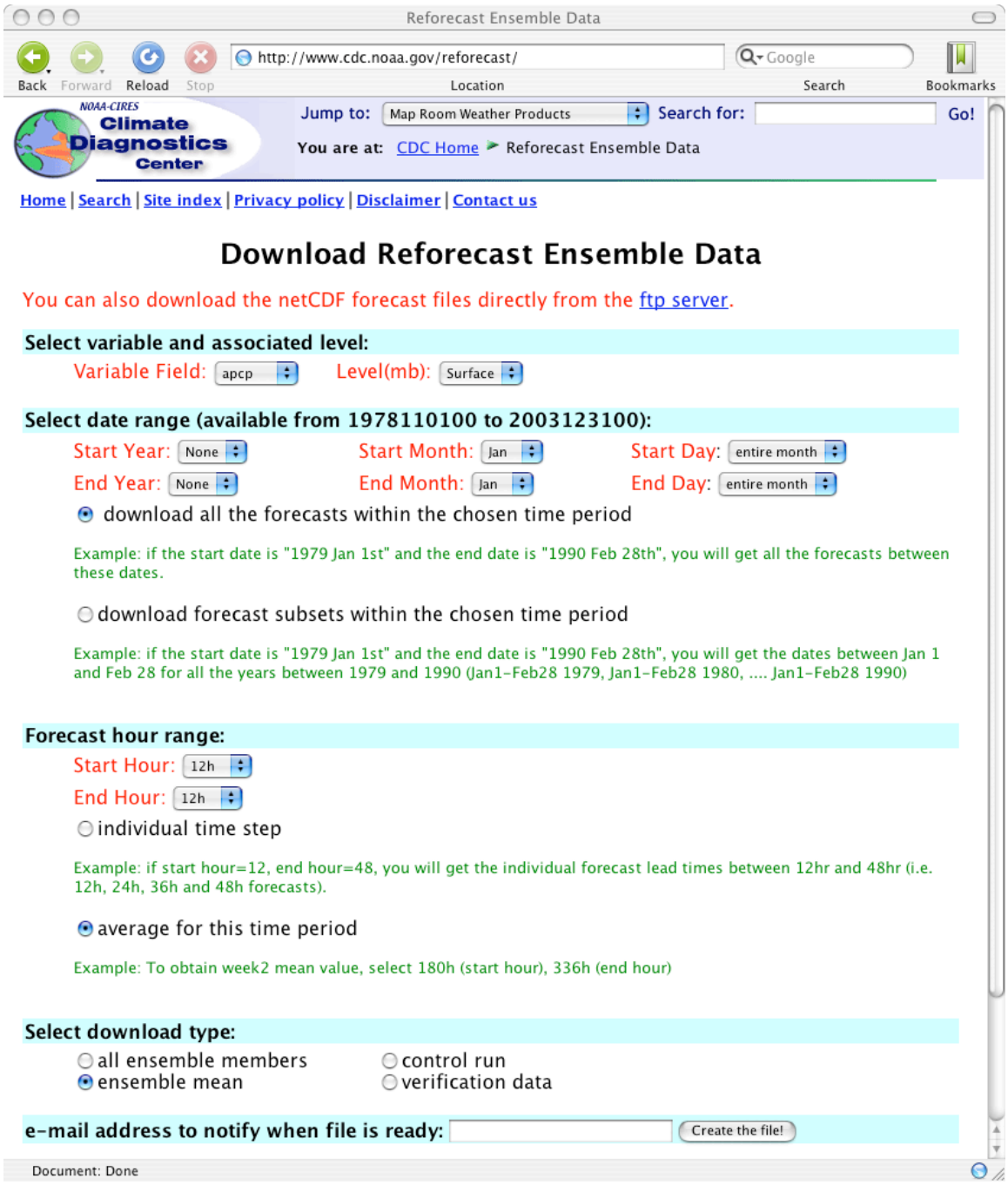

Figure 1: Screenshot of the reforecast data set download web page.

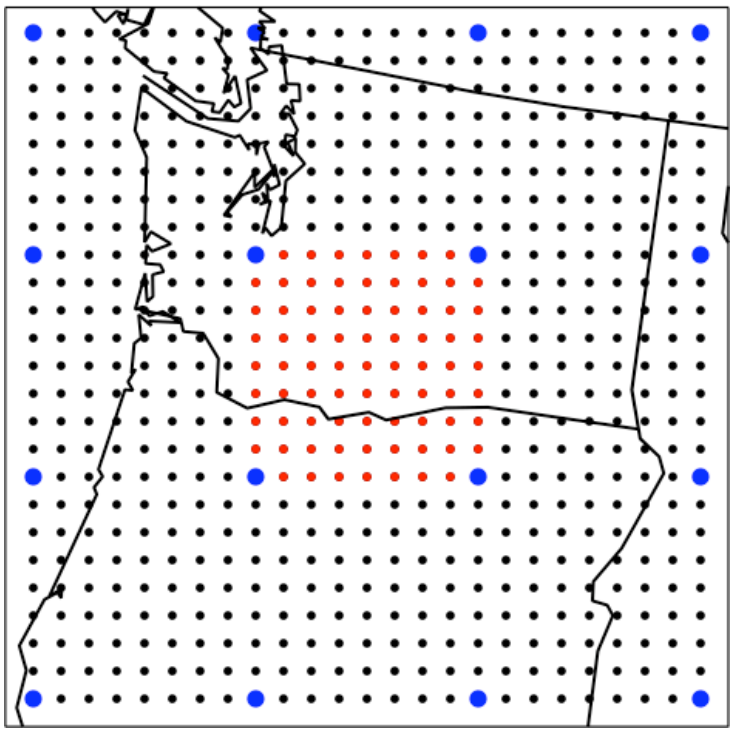

Figure 2: Map of reforecast grid points used in determination of closest analog forecasts. The smaller dots denote where NARR data is available (a 32 km Lambert Conformal grid). Large blue dots denote where the T62 forecasts are available (interpolated from a global 2.5 degree grid to every eighth NARR grid point). The analyzed fields associated with the closest pattern matches at the blue dots are extracted at the red dots. The national forecast is then comprised of a tiling of similar regions from around the country.

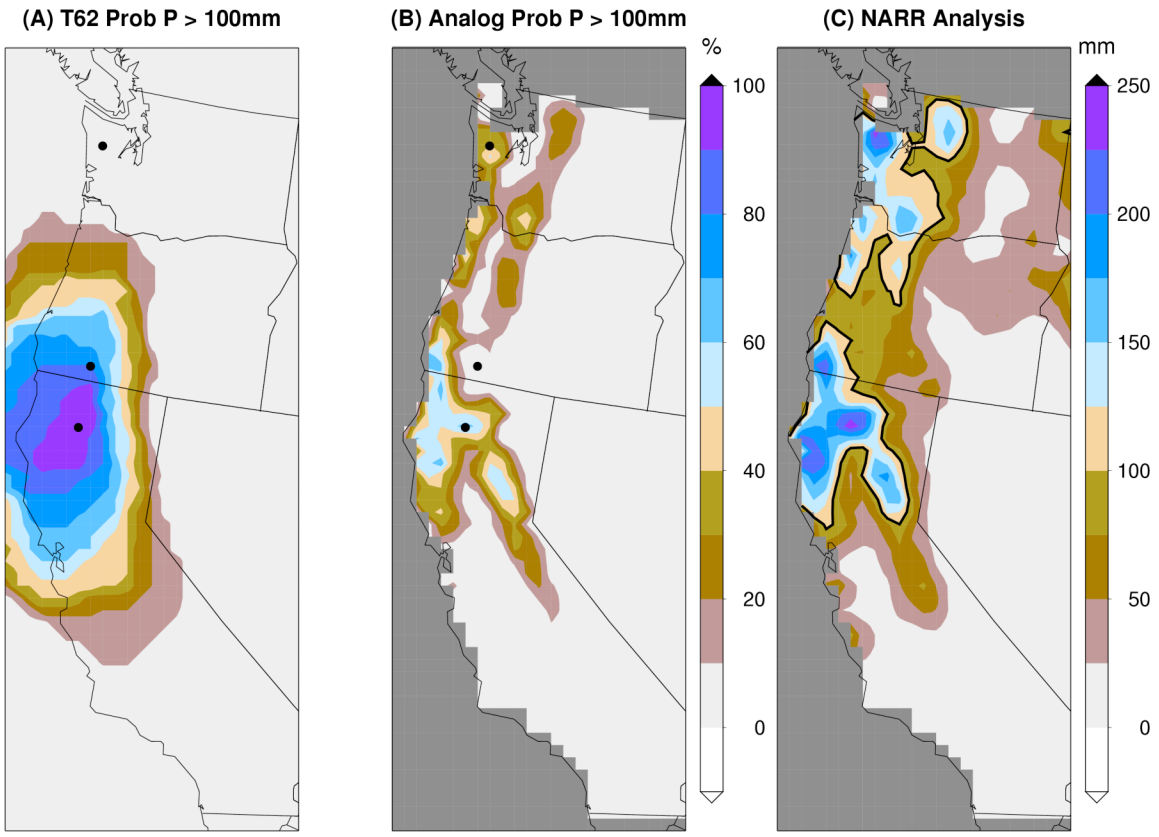

Figure 3: (a) Raw ensemble-based probability of greater than 100 mm precipitation accumulated during days 4-6 for a forecast initialized 0000 UTC 26 December 1996 (from 0000 UTC 29 December 1996 to 0000 UTC 1 January 1997). Dots indicate locations used in Fig. 4. (b) As in (a), but where probabilities have been estimated from relative frequency of historical NARR analogs. (c) Observed precipitation from NARR (mm). 100 mm threshold highlighted.

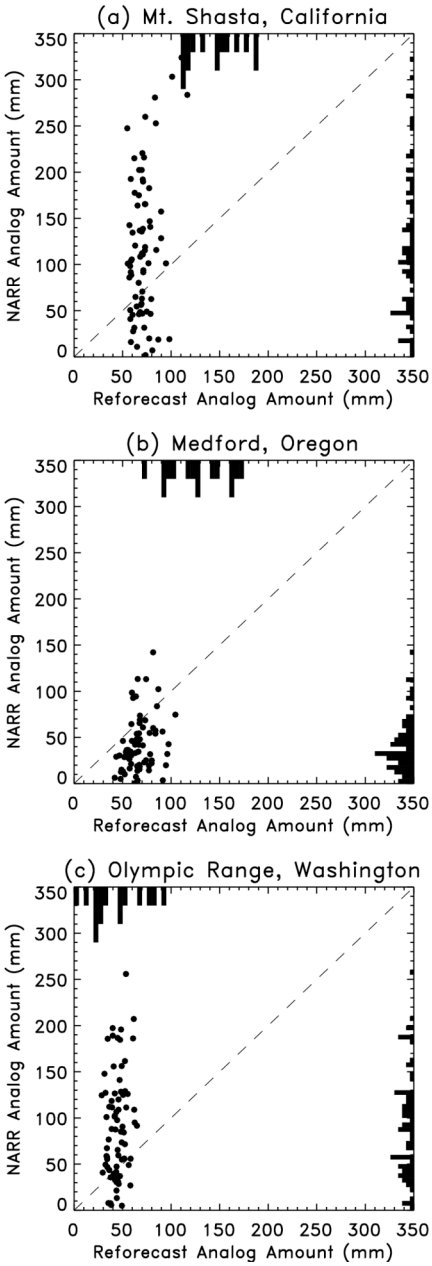

Figure 4: Ensemble forecast, reforecast analog, and observed analog data for three dots in Fig. 3a. Histograms along tops of plots indicate the raw T62 ensemble forecast total amounts. Histograms along right of plots indicate the frequency of NARR analog forecast amounts. Scatterplots indicate the joint value of ensemble-mean analog forecasts taken from the reforecast data set (abscissa) and the value of the associated NARR historical analog (ordinate). (a) Scatterplot from Mt. Shasta (northern California), (b) scatterplot from Medford (southern Oregon), (c) scatterplot from Olympic Mountains, Washington.

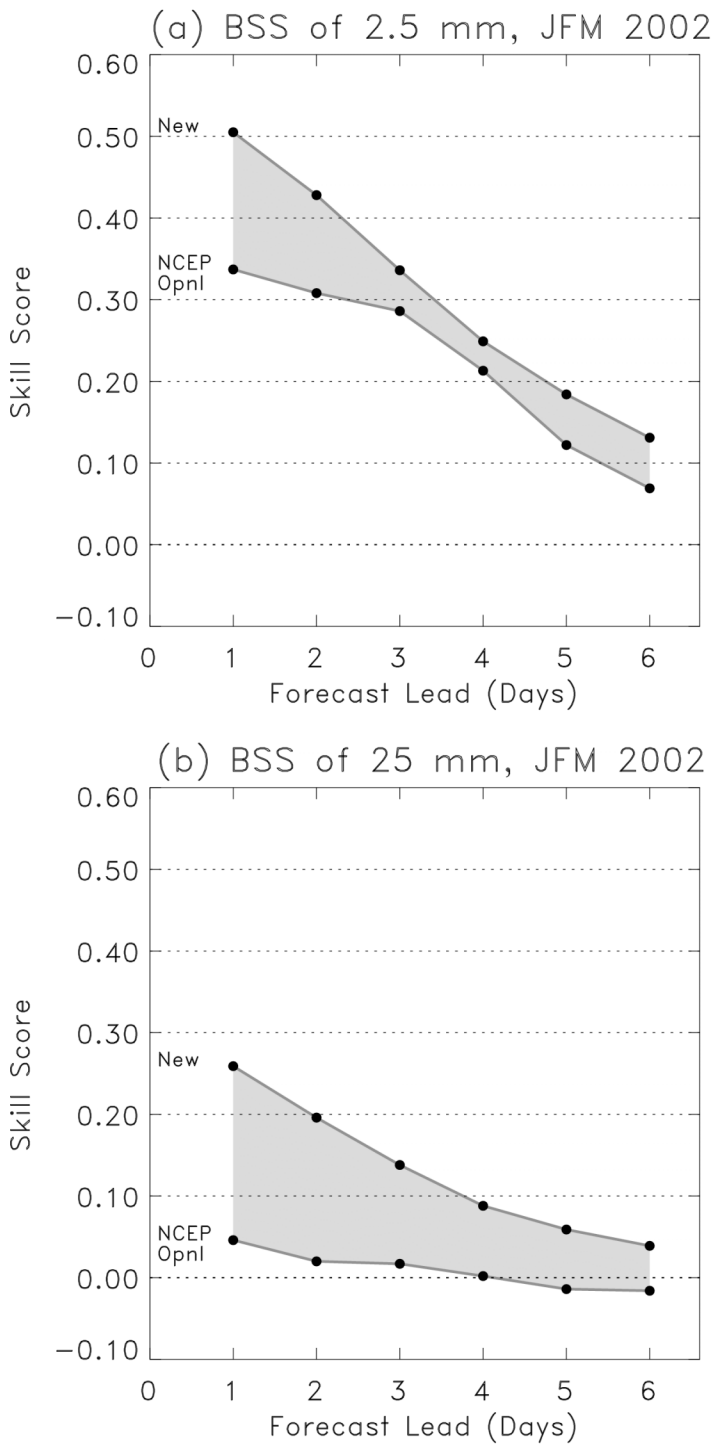

Figure 5: Brier Skill Score of 75-member analog and NCEP ensemble forecasts measured relative to climatology. (a) 2.5 mm skill, (b) 25 mm skill.

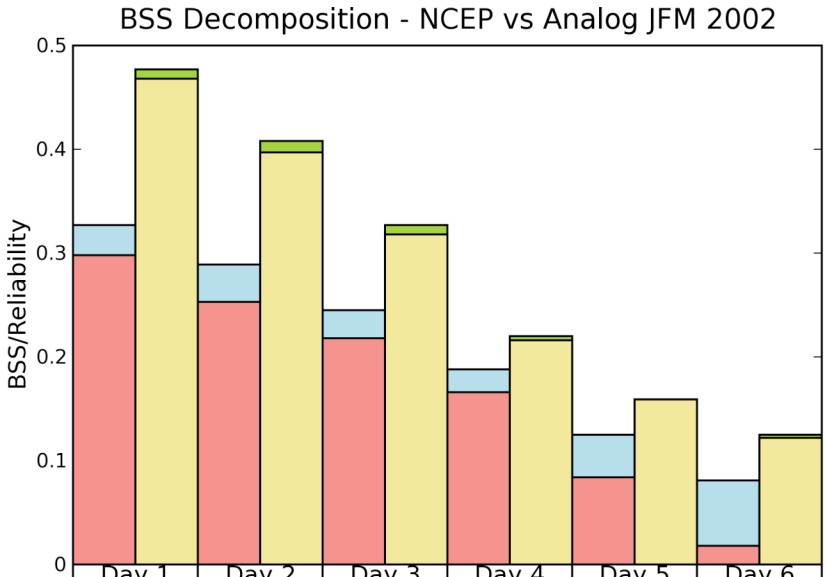

	Day 1	Day 2	Day 3	Day 4	Day 5	Day 6
NCEP BSS	0.298	0.253	0.218	0.166	0.084	0.018
Analog BSS	0.468	0.397	0.318	0.216	0.159	0.122
NCEP Resolution	0.327	0.289	0.245	0.188	0.125	0.081
Analog Resolution	0.477	0.408	0.327	0.220	0.159	0.125
NCEP Reliability	0.029	0.036	0.027	0.022	0.041	0.063
Analog Reliability	0.009	0.011	0.009	0.004	0.000	0.003

Figure 6: Reliability and resolution (scaled by the uncertainty), and Brier Skill Score (BSS) of the probability of precipitation occurring in the upper quintile of the climatological distribution, both for NCEP and 75-member analog forecasts. The overall height of the bar for each day indicates the resolution, NCEP on the left and analogs on the right. NCEP reliability is colored blue, analog reliability is colored green, NCEP BSS is red, and analog BSS is yellow.

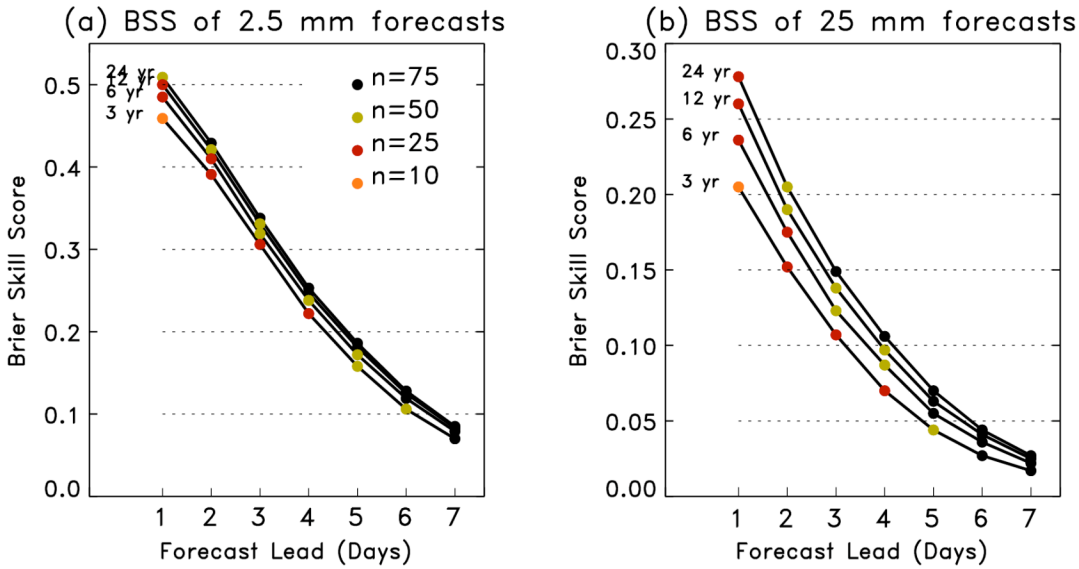

Figure 7: Brier Skill Scores of the analog reforecast technique for various lengths of the training data set. Probabilistic forecasts were calculated for ensembles of size 10, 25, 50, and 75; the skill of the ensemble size that was most skillful is the only one plotted. The color of the dot denotes the size of the most skillful ensemble that was plotted.

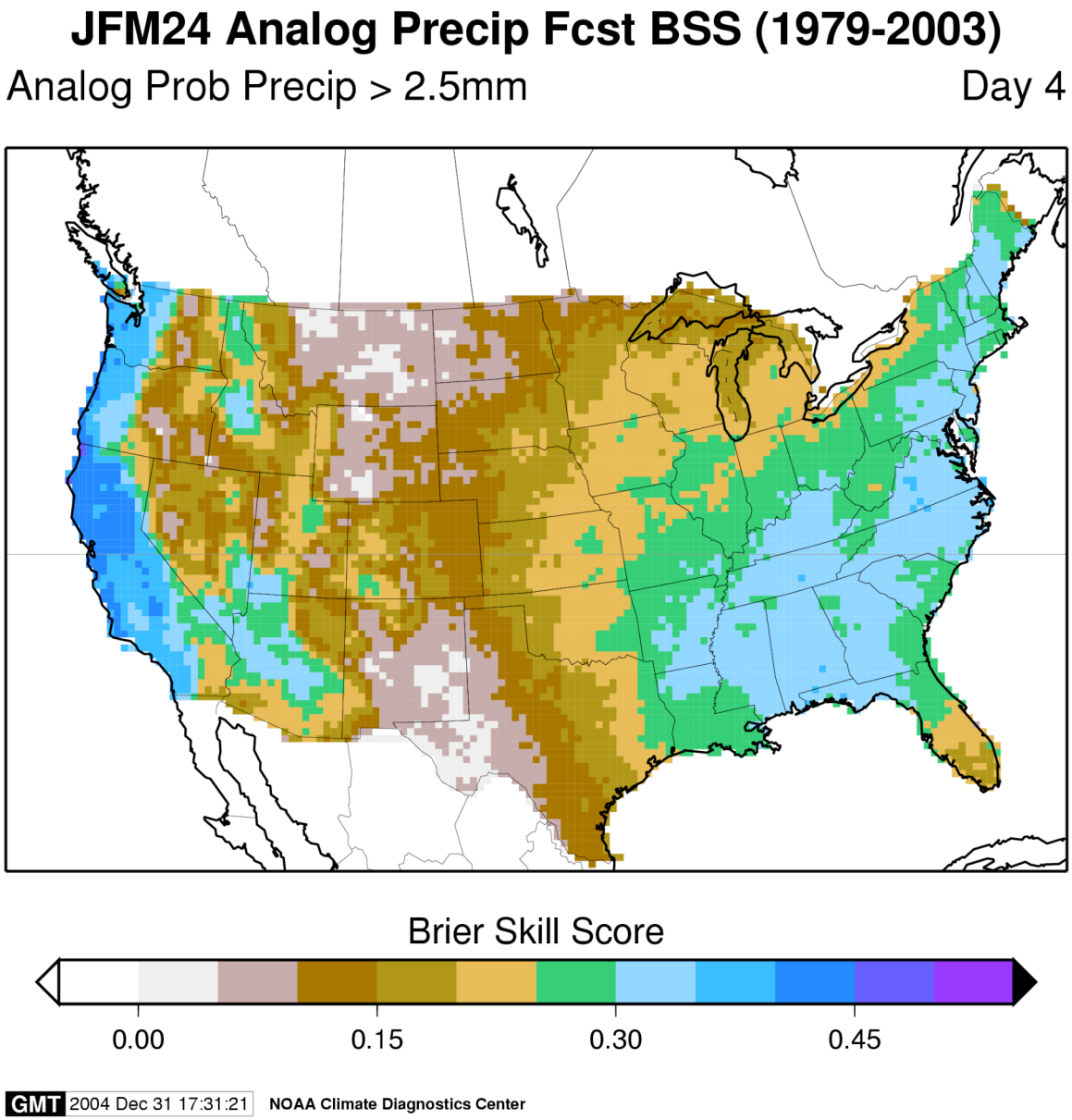

Figure 8: Map of Brier Skill Scores of 24-h accumulated precipitation forecasts between 3 and 4 days lead at 2.5 mm threshold for JFM 1979-2002.

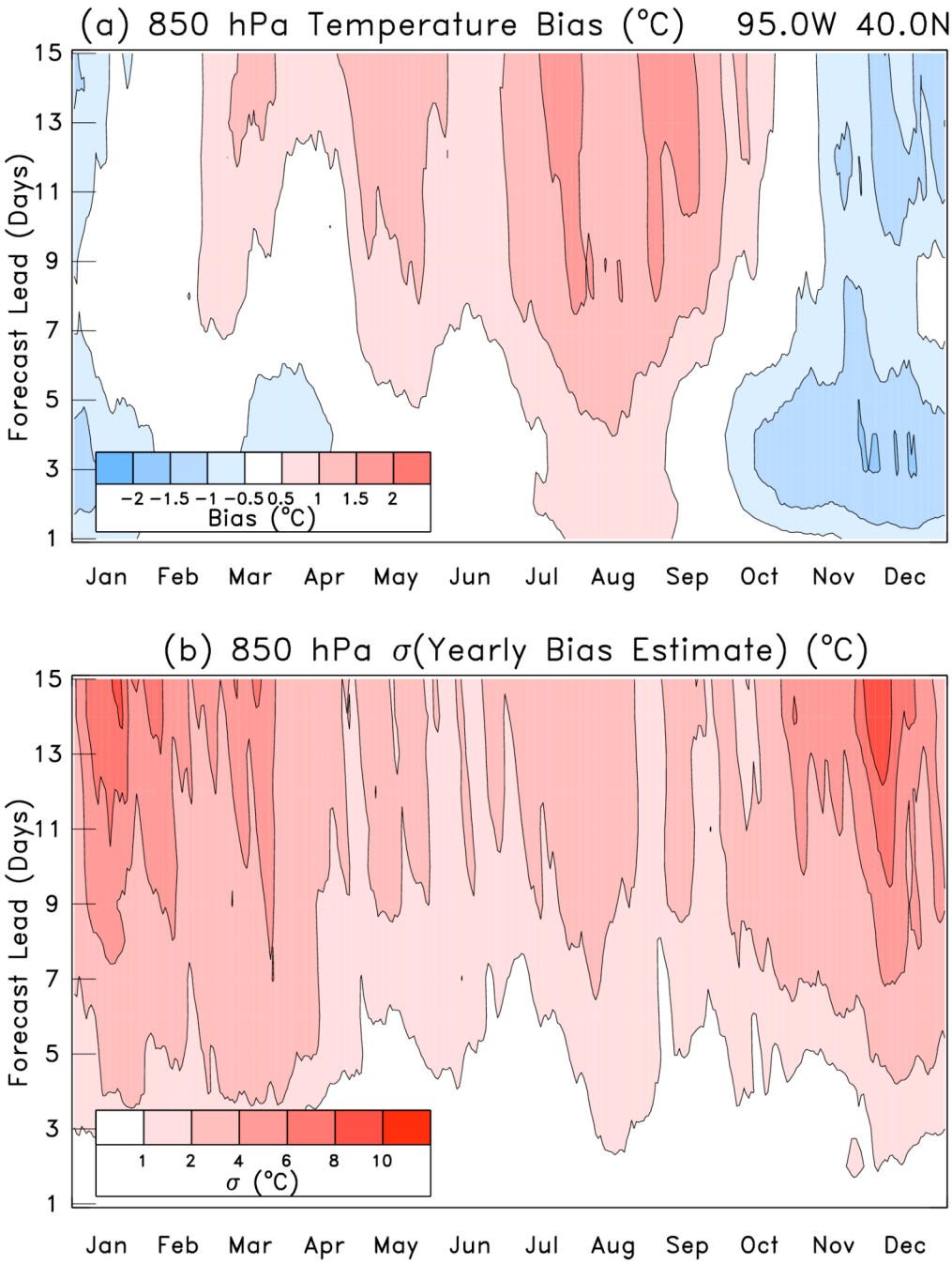

Figure 9: (a) 850 hPa temperature bias at -95.0 W, 40.0 N, as a function of time of year and forecast lead. (b) Standard deviation of the yearly bias estimates.

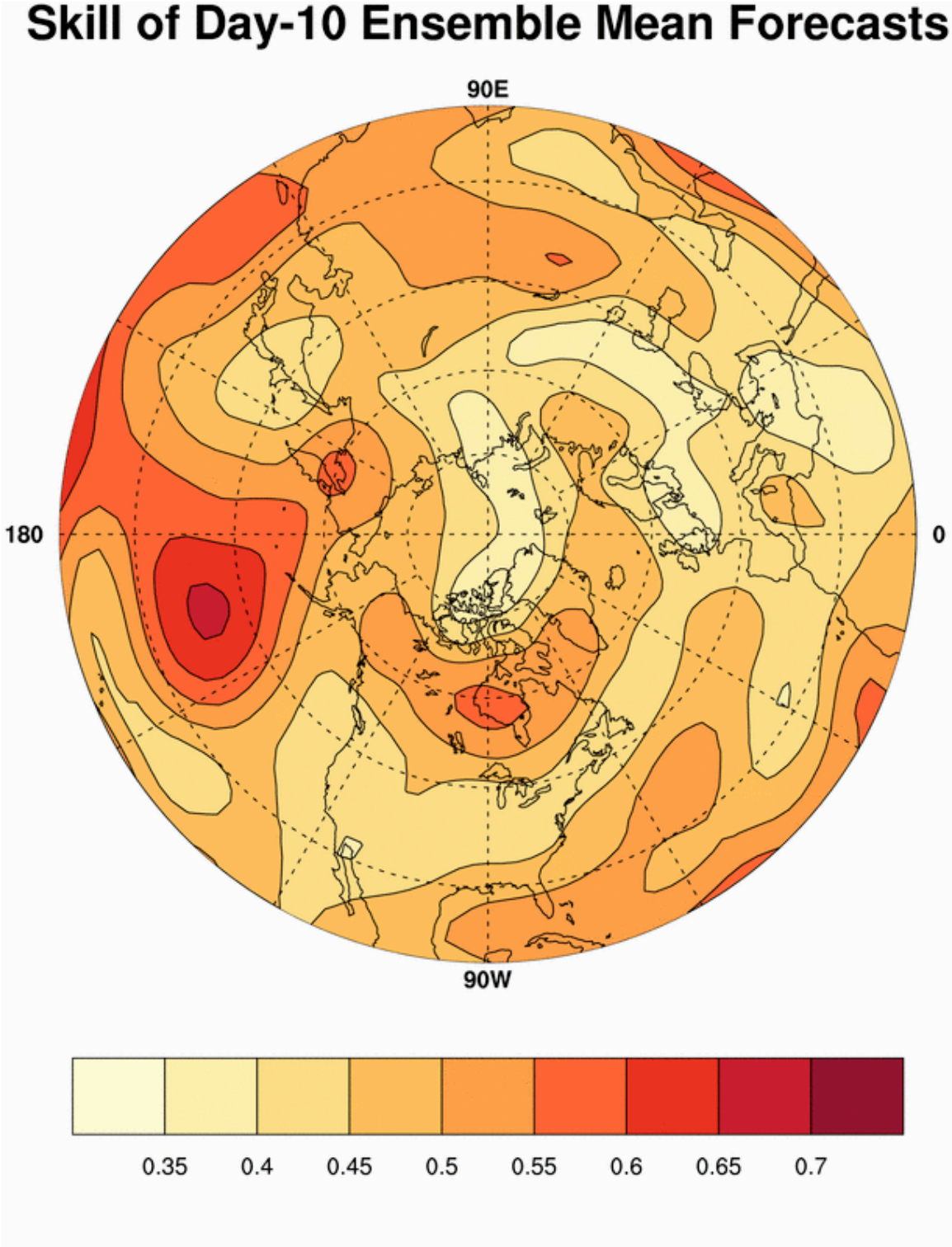

Figure 10: Correlation between time series of ensemble mean day-10 forecasts and corresponding verifying analyses (from the NCEP/NCAR reanalysis) at every grid point in the Northern Hemisphere for December to February 1979-2003.

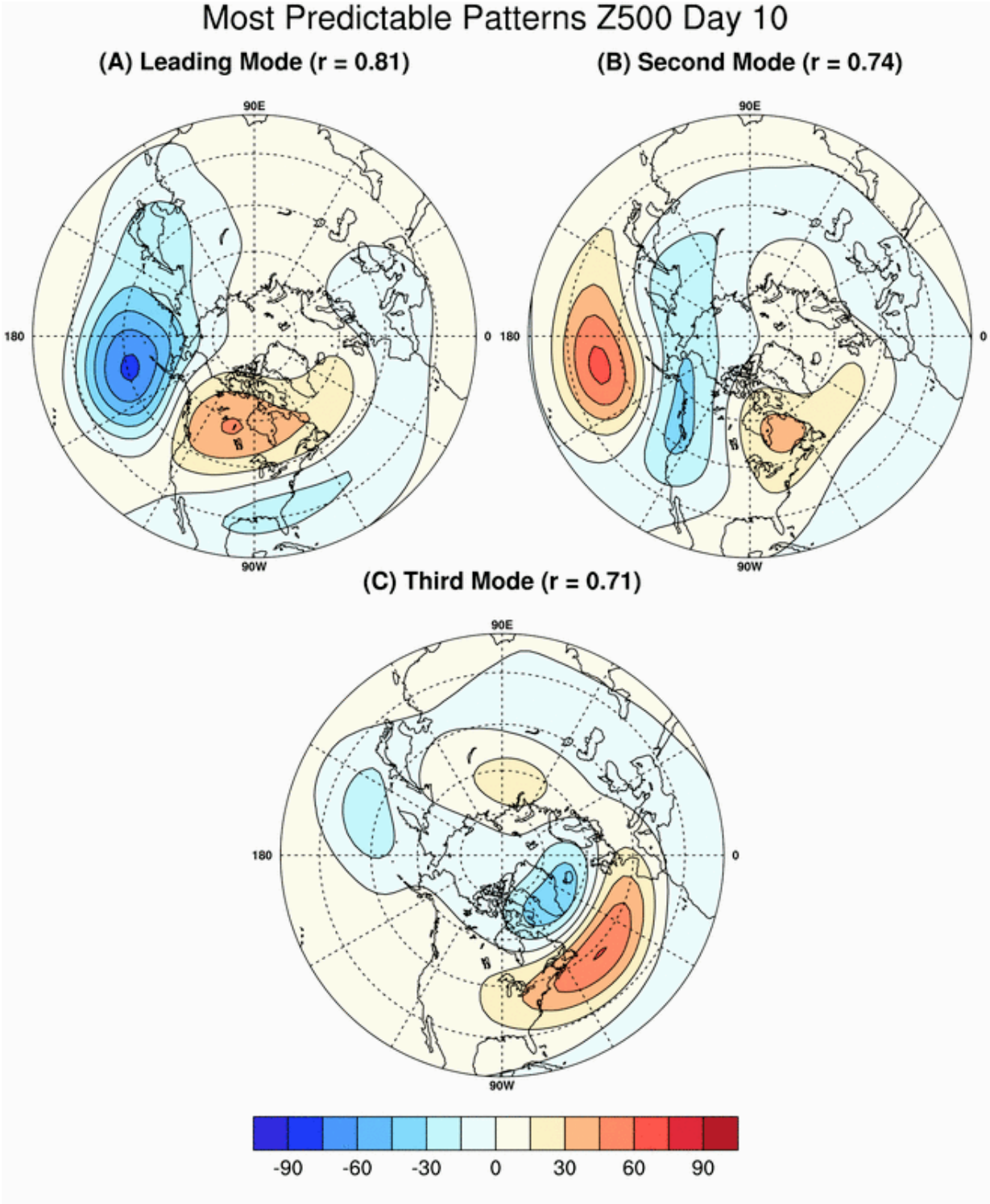

Figure 11 : Ensemble mean day-10 forecast 500 hPa height regressed on to the time series of the three most predictable forecast patterns. Contour interval 15 m. The correlation of between the time series of the predictor pattern and the corresponding predictand pattern (*r*) is given for each pattern.

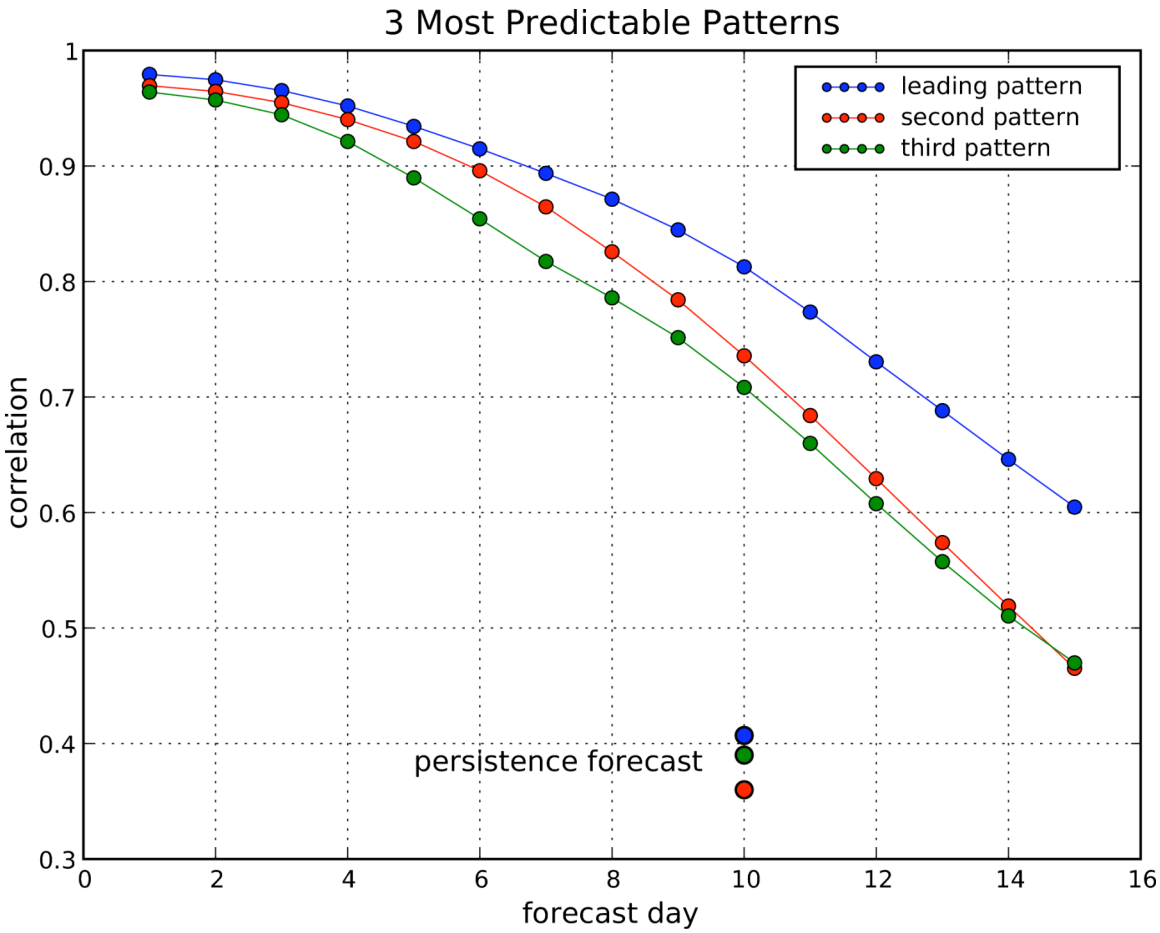

Figure 12: Correlation between the time series of the first three most predictable 500 hPa height day 10 forecast patterns and the time series of the corresponding patterns in the verifying analyses as a function of forecast lead time. The three dots labeled 'persistence forecast' indicate the skill of a forecast which persists the projections in the day 1 forecast to day 10.